

# Chemical and structural properties of the system $\text{Fe}_2\text{O}_3\text{--Nd}_2\text{O}_3$

S. MUSIĆ, S. POPOVIĆ\*, M. RISTIĆ

*Ruđer Bošković Institute, P.O. Box 1016, 41001 Zagreb, \*and also Department of Physics, Faculty of Science, P.O. Box 162, 41001 Zagreb, Croatia*

B. SEPIOL

*Institut für Festkörperphysik der Universität Wien, Strudlhofgasse 4, A-1090 Vienna, Austria*

Chemical and structural properties of the system  $(1-x)\text{Fe}_2\text{O}_3 + x\text{Nd}_2\text{O}_3$ ,  $0 \leq x \leq 1$ , were investigated using X-ray diffraction,  $^{57}\text{Fe}$  Mössbauer spectroscopy and Fourier transform–infrared (FT–IR) spectroscopy. The samples were prepared by the chemical coprecipitation and thermal treatment of  $\text{Fe}(\text{OH})_3/\text{Nd}(\text{OH})_3$  coprecipitates. X-ray diffraction showed the presence of oxide phases  $\alpha\text{-Fe}_2\text{O}_3 + \text{NdFeO}_3$  in the  $\text{Fe}_2\text{O}_3$ -rich region, and the oxide phases  $\text{Nd}_2\text{O}_3 + \text{NdFeO}_3$  in the  $\text{Nd}_2\text{O}_3$ -rich region.  $^{57}\text{Fe}$  Mössbauer spectra were characterized with one sextet of spectral lines at room temperature. Mathematical evaluation of the Mössbauer spectra showed distinct regularities in the changes of Mössbauer parameters, thus indicating the presence of two subspectra with very similar spectral behaviour. High sensitivity of the  $\text{Nd}_2\text{O}_3$  phase to the moisture and atmosphere  $\text{CO}_2$  was demonstrated by FT–IR spectroscopy.

## 1. Introduction

Mixed metal oxides have found important application in advanced technologies, such as ferroelectrics, ferrites, sensors, magneto-optical readers, catalysts, etc. In practice they can be applied as chemical compounds, in which the metal cations possess exact positions in the oxide crystal structure, as solid solutions or as composite materials. Significant attention has been directed towards the mixed metal oxides, after the discovery that some of them exhibited high-temperature superconductivity. Mixed metal oxides can be prepared using the chemical coprecipitation and thermal treatment of hydroxide coprecipitates, or using sol–gel procedure, thermal decomposition of metal-organic salts, ceramic sintering, crystal growth from melt, or film growth on different substrates. Chemical and structural properties of the mixed metal oxides are dependent on the experimental conditions of their synthesis. Mössbauer spectroscopy has found important application in the study of structural and magnetic properties of the mixed metal oxides containing iron and/or rare-earth cations [1].

Ristić *et al.* [2] used X-ray diffraction and Mössbauer spectroscopy of  $^{151}\text{Eu}$  and  $^{57}\text{Fe}$  to characterize the samples prepared in the system  $(1-x)\text{Fe}_2\text{O}_3 + x\text{Eu}_2\text{O}_3$ ,  $0 \leq x \leq 1$ . The samples were prepared using chemical coprecipitation and thermal treatment of hydroxide coprecipitates. A sequence of oxide phases,  $\alpha\text{-Fe}_2\text{O}_3$ ,  $\text{Eu}_3\text{Fe}_5\text{O}_{12}$ ,  $\text{EuFeO}_3$  and  $\text{Eu}_2\text{O}_3$  was detected at different values of  $x$ . Poorly crystallized material and/or amorphous fraction were observed in samples prepared at 600 °C. When the heating temperature was increased to 900 °C, the

amorphous fraction disappeared and all the samples were well crystallized.

Musić *et al.* [3] investigated the formation of oxide phases in the system  $(1-x)\text{Fe}_2\text{O}_3 + x\text{Gd}_2\text{O}_3$ . The samples were also prepared using the chemical coprecipitation method. A distribution of oxide phases,  $\alpha\text{-Fe}_2\text{O}_3$ ,  $\text{Gd}_3\text{Fe}_5\text{O}_{12}$ ,  $\text{GdFeO}_3$  and  $\text{Gd}_2\text{O}_3$  was determined, as a function of  $x$ . The temperature of the solid-state synthesis of  $\text{Gd}_3\text{Fe}_5\text{O}_{12}$  [4] was significantly higher than the temperatures of formation of  $\text{Eu}_3\text{Fe}_5\text{O}_{12}$  and  $\text{Gd}_3\text{Fe}_5\text{O}_{12}$ , which were prepared using the chemical coprecipitation [2, 3]. In these oxide systems, no solid solutions were observed with certainty, even at the very ends of the concentration range. New accurate crystallographic data were determined for  $\text{Gd}_3\text{Fe}_5\text{O}_{12}$  [3].

The aim of the present work was to obtain new information about the formation of oxide phases in the system  $\text{Fe}_2\text{O}_3\text{--Nd}_2\text{O}_3$ . It is known that  $\text{Nd}^{3+}$  shows different chemical behaviour in relation to  $\text{Eu}^{3+}$  or  $\text{Gd}^{3+}$ . Oxide samples were prepared using the chemical coprecipitation and thermal treatment of hydroxide coprecipitates. X-ray diffraction,  $^{57}\text{Fe}$  Mössbauer spectroscopy and Fourier transform–IR (FT–IR) spectroscopy were used as experimental techniques.

## 2. Experimental procedure

The samples were prepared using the chemical coprecipitation method. Mixed metal hydroxides,  $\text{Fe}(\text{OH})_3/\text{Nd}(\text{OH})_3$ , were coprecipitated from the corresponding nitrate solutions. The hydroxide

coprecipitates, were cleaned from "neutral" electrolyte with doubly distilled water using a Sorvall RC2-B superspeed centrifuge (up to 20 000 r.p.m.). The wet samples were dried in vacuum at room temperature. The hydroxide coprecipitates were thermally treated for 1 h at 200 °C, 1 h at 300 °C, 1 h at 500 °C, 1 h at 600 °C and 4 h at 900 °C. Samples, FN-6 to FN-12 were additionally heated for 2 h at 900 °C. The chemical composition of the samples,  $(1-x)\text{Fe}_2\text{O}_3 + x\text{Nd}_2\text{O}_3$ , is given in Table I.

X-ray powder diffraction (XRD) measurements were performed at room temperature using a Philips counter diffractometer with monochromatized  $\text{CuK}\alpha$  radiation (graphite monochromator).

$^{57}\text{Fe}$  Mössbauer spectra were recorded using the spectrometer made by Halder Elektronik GmbH. Mössbauer spectra were evaluated using a Mössbauer fitting program written by Ruebenbauer and Birchall [5].

FT-IR spectra were recorded at room temperature using the Perkin-Elmer spectrometer. The FT-IR spectrometer was coupled to a personal computer loaded with an IR Data Manager (IRDM) program. The samples were pressed into discs using spectroscopically pure KBr.

### 3. Results and discussion

The results of XRD phase analysis of the samples prepared in the system  $(1-x)\text{Fe}_2\text{O}_3 + x\text{Nd}_2\text{O}_3$  are summarized in Table II. As the initial molar content of  $\text{Nd}_2\text{O}_3$  increased from sample FN-1 to sample FN-7, the molar fraction of  $\text{NdFeO}_3$  increased, while the fraction of  $\alpha\text{-Fe}_2\text{O}_3$  decreased. The maximum fraction of  $\text{NdFeO}_3$  was observed in sample FN-8, and it decreased up to sample FN-11.  $\alpha\text{-Fe}_2\text{O}_3$  was not detected in samples FN-8 to FN-11.  $\text{Nd}_2\text{O}_3$  was observed in sample FN-8, and its fraction increased up to sample FN-12. Sample FN-12 corresponded to pure  $\text{Nd}_2\text{O}_3$ . Samples FN-8 to FN-12, prepared for XRD measurements, were immersed in oil after their calcination and cooling to room temperature. This was done to avoid the reaction between  $\text{Nd}_2\text{O}_3$  and atmospheric moisture.

Table III shows  $^{57}\text{Fe}$  Mössbauer parameters (RT) calculated on the basis of the spectra recorded for the

TABLE I Chemical composition of the samples prepared in the system  $(1-x)\text{Fe}_2\text{O}_3 + x\text{Nd}_2\text{O}_3$

Sample	Molar fraction	
	$\text{Fe}_2\text{O}_3$ (1-x)	$\text{Nd}_2\text{O}_3$ (x)
FN-1	0.99	0.01
FN-2	0.97	0.03
FN-3	0.95	0.05
FN-4	0.90	0.10
FN-5	0.85	0.15
FN-6	0.80	0.20
FN-7	0.70	0.30
FN-8	0.50	0.50
FN-9	0.30	0.70
FN-10	0.10	0.90
FN-11	0.05	0.95
FN-12	0	1

TABLE II The results of X-ray diffraction phase analysis of samples FN-1 to FN-12

Sample	Phase composition (approx. molar fraction)
FN-1	$\alpha\text{-Fe}_2\text{O}_3 + \text{NdFeO}_3$ (0.02)
FN-2	$\alpha\text{-Fe}_2\text{O}_3 + \text{NdFeO}_3$ (0.06)
FN-3	$\alpha\text{-Fe}_2\text{O}_3 + \text{NdFeO}_3$ (0.10)
FN-4	$\alpha\text{-Fe}_2\text{O}_3 + \text{NdFeO}_3$ (0.20)
FN-5	$\alpha\text{-Fe}_2\text{O}_3 + \text{NdFeO}_3$ (0.30)
FN-6	$\alpha\text{-Fe}_2\text{O}_3 + \text{NdFeO}_3$ (0.40)
FN-7	$\text{NdFeO}_3 + \alpha\text{-Fe}_2\text{O}_3$ (0.40)
FN-8	$\text{NdFeO}_3 + \text{Nd}_2\text{O}_3$ (0.10)
FN-9	$\text{Nd}_2\text{O}_3 + \text{NdFeO}_3$ (0.50)
FN-10	$\text{Nd}_2\text{O}_3 + \text{NdFeO}_3$ (0.20)
FN-11	$\text{Nd}_2\text{O}_3 + \text{NdFeO}_3$ (0.10)
FN-12	$\text{Nd}_2\text{O}_3$

samples  $(1-x)\text{Fe}_2\text{O}_3 + x\text{Nd}_2\text{O}_3$ . For illustration, Figs 1 and 2 show  $^{57}\text{Fe}$  Mössbauer spectra of samples FN-6 and FN-9, recorded at room temperature. Hyperfine magnetic splitting is the main characteristic of the  $^{57}\text{Fe}$  Mössbauer spectra of samples FN-1 to FN-11. In samples FN-1 to FN-7, X-ray diffraction showed the presence of  $\alpha\text{-Fe}_2\text{O}_3$  and  $\text{NdFeO}_3$  which are known to exhibit hyperfine magnetic splitting at room temperature. On the basis of this fact, two separable sextets were expected.  $^{57}\text{Fe}$  Mössbauer spectra of samples FN-1 to FN-7 showed only the presence of one sextet. However, after the mathematical evaluation of these spectra, distinct regularities in the changes of the  $^{57}\text{Fe}$  Mössbauer parameters, from sample FN-1 to sample FN-11, were observed.

The hyperfine magnetic field,  $\text{HMF} = 516 \text{ kOe}$ , and quadrupole splitting,  $\Delta E_q = -0.208 \text{ mm s}^{-1}$ , observed for sample FN-1, can be ascribed to  $\alpha\text{-Fe}_2\text{O}_3$ . In the  $^{57}\text{Fe}$  Mössbauer spectra of samples FN-1 and FN-2 the central quadrupole doublet of very small intensity with splitting ( $\Delta = 1.03 \text{ mm s}^{-1}$ ) was measured. With increase of  $\text{Nd}_2\text{O}_3$  molar content in the samples  $(1-x)\text{Fe}_2\text{O}_3 + x\text{Nd}_2\text{O}_3$ , there is a gradual decrease of HMF value. A gradual change of  $\Delta E_q$  from  $-0.208 \text{ mm s}^{-1}$  for sample FN-1 to  $0 \text{ mm s}^{-1}$  for sample FN-11 was observed. The line width,  $\Gamma$ , increased gradually with the increase of initial  $\text{Nd}_2\text{O}_3$  molar content up to sample FN-5 ( $\Gamma = 0.364 \text{ mm s}^{-1}$ ) and then showed a tendency to decrease, up to sample FN-11. The values of the isomer shift,  $\delta$ , and quadrupole splitting,  $\Delta E_q$ , measured for samples FN-8 to FN-11 can be ascribed to  $\text{NdFeO}_3$ ; however, the measured value of HMF (510–512 kOe) was larger than that reported in the literature for  $\text{NdFeO}_3$ . Eibshütz *et al.* [6] reported the following Mössbauer parameters for  $\text{NdFeO}_3$  at room temperature:  $\delta = 0.10 \text{ mm s}^{-1}$  ( $^{57}\text{Co}/\text{Cu}$ ),  $\Delta E_q = 0.0 \text{ mm s}^{-1}$  and  $\text{HMF} = 506 \text{ kOe}$ . Fig. 3 shows the dependence of  $\Gamma$

TABLE III  $^{57}\text{Fe}$  Mössbauer parameters (RT) calculated on the basis of recorded spectra for the samples prepared in the system  $\text{Fe}_2\text{O}_3\text{-Nd}_2\text{O}_3$

Sample	Lines	Isomer shift $\delta^a$ ( $\text{mm s}^{-1}$ )	Quadrupole splitting, $\Delta E_q$ ( $\text{mm s}^{-1}$ )	Hyperfine magnetic field, HMF ( $\text{mm s}^{-1}$ )	Line width, $\Gamma$ ( $\text{mm s}^{-1}$ )
FN-1	Q	0.304	1.030		0.300
	M	0.367	-0.208	516	0.319
FN-2	Q	0.306	1.030		0.300
	M	0.369	-0.207	515.9	0.322
FN-3	M	0.370	-0.205	515.7	0.350
FN-4	M	0.370	-0.194	514.8	0.350
FN-5	M	0.369	-0.180	514.5	0.364
FN-6	M	0.369	-0.168	515.1	0.324
FN-7	M	0.368	-0.131	514.7	0.338
FN-8	M	0.372	-0.0	510.3	0.308
FN-9	M	0.370	-0.0	511.1	0.314
FN-10	M	0.381	-0.0	511.9	0.286
FN-11	M	0.369	-0.0	511.8	0.308

<sup>a</sup> Isomer shift is given relative to  $\alpha\text{-Fe}$ .

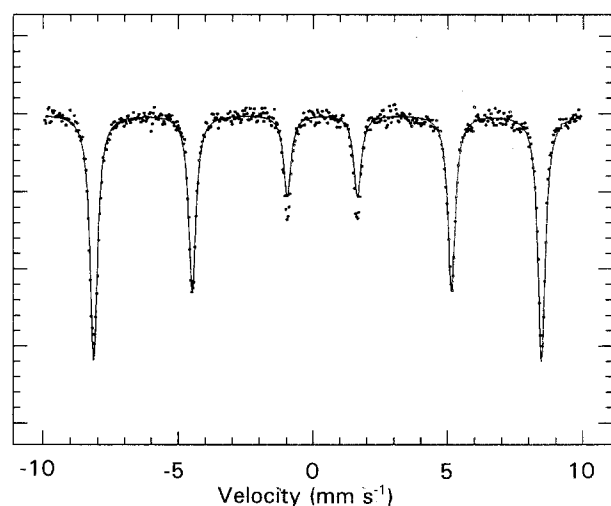


Figure 1  $^{57}\text{Fe}$  Mössbauer spectrum of sample FN-6, recorded at room temperature.

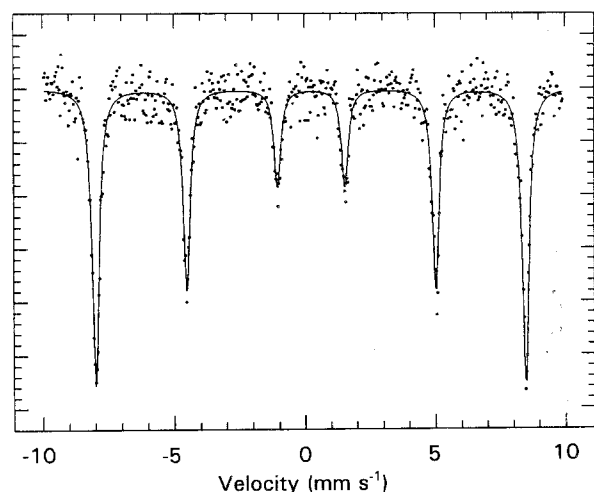


Figure 2  $^{57}\text{Fe}$  Mössbauer spectrum of sample FN-9, recorded at room temperature.

and  $\Delta E_q$  on the molar contents of  $\text{Nd}_2\text{O}_3$  and  $\text{Fe}_2\text{O}_3$  in the samples  $(1-x)\text{Fe}_2\text{O}_3 + x\text{Nd}_2\text{O}_3$ .

The FT-IR spectrum of sample FN-1, shown in Fig. 4, is characterized by two dominant bands at 554

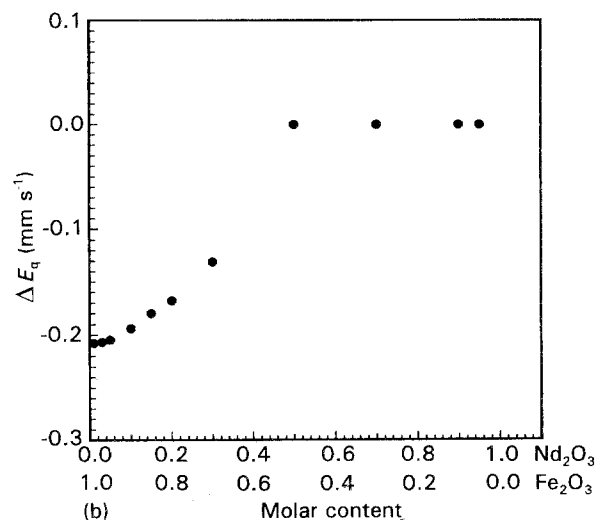
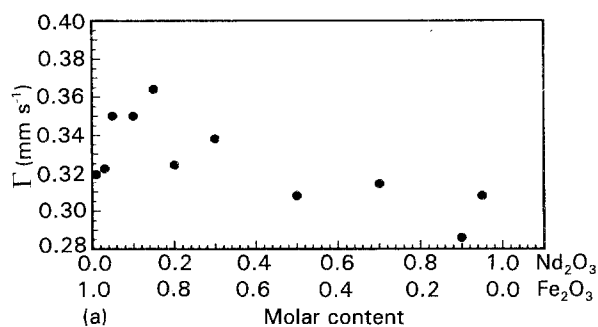


Figure 3 The dependence (at RT) of (a) line width,  $\Gamma$ , and (b) quadrupole splitting,  $\Delta E_q$ , on the molar content of  $\text{Nd}_2\text{O}_3$  and  $\text{Fe}_2\text{O}_3$ , respectively.

and  $472\text{ cm}^{-1}$ , a band at  $389\text{ cm}^{-1}$  and two shoulders at  $638$  and  $438\text{ cm}^{-1}$ . These IR bands correspond to  $\alpha\text{-Fe}_2\text{O}_3$ . The IR spectrum of  $\alpha\text{-Fe}_2\text{O}_3$  was discussed in previous papers [7, 8]. With the increase of  $\text{Nd}_2\text{O}_3$  molar content in the samples  $(1-x)\text{Fe}_2\text{O}_3 + x\text{Nd}_2\text{O}_3$ , a gradual formation of a band at  $436\text{ cm}^{-1}$  was observed. This IR band can be related to the perovskite structure [4], in the present case with  $\text{NdFeO}_3$ .

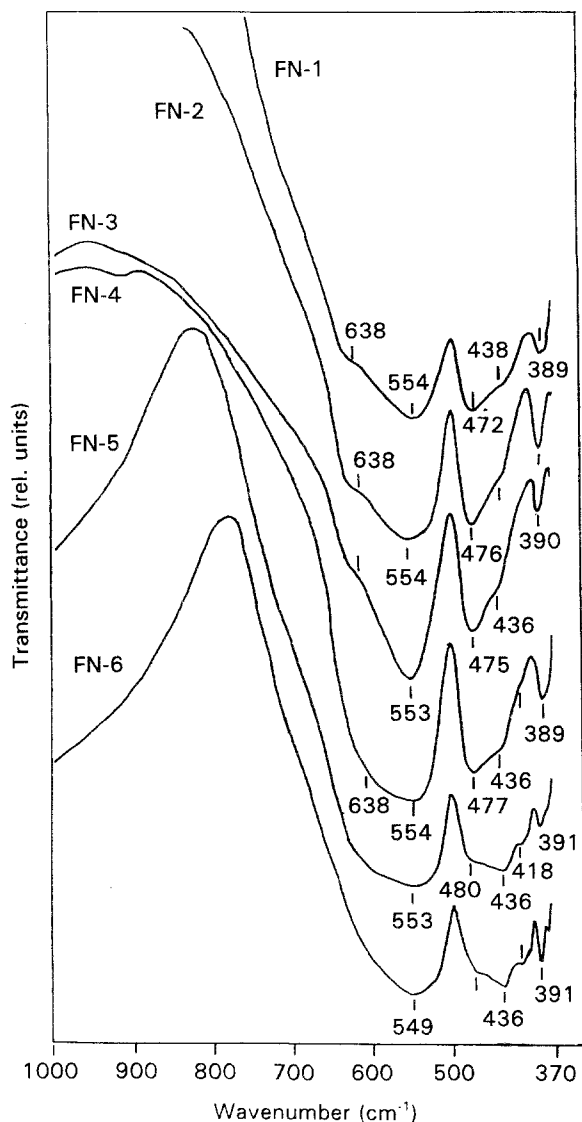


Figure 4 FT-IR spectra of samples FN-1 to sample FN-6, recorded at room temperature.

In the present investigation, a very high sensitivity of  $\text{Nd}_2\text{O}_3$  to moisture and carbon dioxide was observed. This can be illustrated by the FT-IR spectra of samples FN-7 to FN-11, exposed to the atmosphere for a prolonged time. In Fig. 5 these samples are denoted by an asterisk. XRD showed the presence of  $\text{Nd}(\text{OH})_3$  in samples FN-8\* to FN-11\*, and its fraction increased from sample FN-8\* to FN-11\*. The FT-IR spectrum of sample FN-7\* is characterized with two bands at 564 and 436  $\text{cm}^{-1}$ , with shoulders at 674, 477 and 418  $\text{cm}^{-1}$ . On the basis of the FT-IR spectrum of sample FN-7\* it can be concluded that this sample does not contain  $\text{Nd}(\text{OH})_3$ . XRD analysis showed the presence of  $\text{NdFeO}_3$  (0.60) and  $\alpha\text{-Fe}_2\text{O}_3$  (0.40) in sample FN-7\*. The FT-IR spectrum of sample FN-8\* showed a sharp peak at 3606  $\text{cm}^{-1}$  and bands at 1513, 1398 and 674  $\text{cm}^{-1}$ . The bands at 3606 and 674  $\text{cm}^{-1}$  can be ascribed to  $\text{Nd}(\text{OH})_3$ , while bands at 1513 and 1398  $\text{cm}^{-1}$  are due to the presence of carbonates adsorbed by  $\text{Nd}(\text{OH})_3$ . The intensities of IR bands at 3606 and 674  $\text{cm}^{-1}$  increased as the fraction of  $\text{Nd}(\text{OH})_3$  increased from sample FN-8\* to sample FN-11\*. Sample FN-12 transformed to

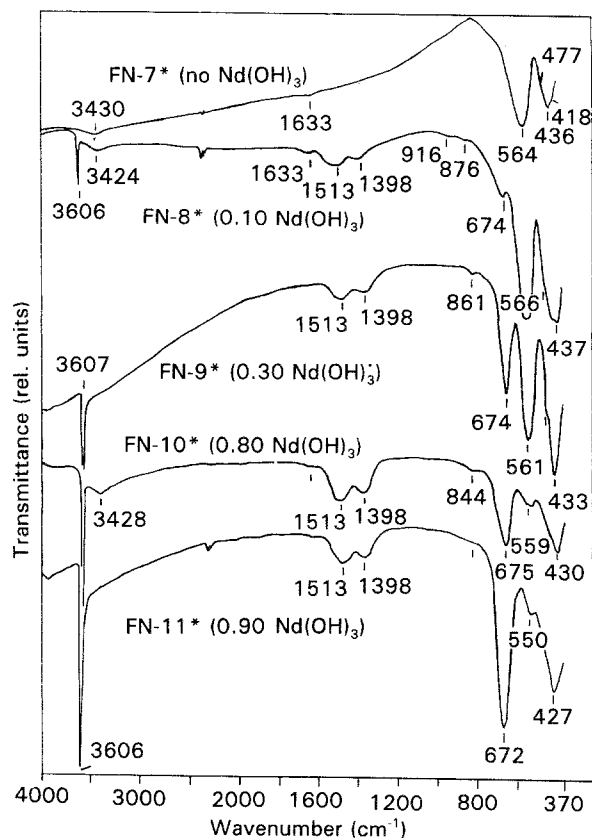


Figure 5 FT-IR spectra of samples FN-7\* to FN-11\*, recorded at room temperature.

$\text{Nd}(\text{OH})_3$  (sample FN-12\*) after exposure to the atmosphere for a prolonged time.

Generally, lanthanide hydroxides are very sensitive to adsorption of atmospheric  $\text{CO}_2$ . Lanthanide cations also show a strong tendency to form basic carbonates [9-12].

Fig. 6 shows the FT-IR spectrum of a sample as-received from Trona, Lindsay Chemical Corporation, West Chicago, IL, and declared to be  $\text{Nd}_2\text{O}_3$ . Fig. 6 also shows the FT-IR spectrum of this sample, recorded immediately after calcination at 900  $^\circ\text{C}$  for 2 h. It is obvious that the Trona sample was dominantly  $\text{Nd}(\text{OH})_3$  with adsorbed carbonates, which was also proved by XRD. After calcination, the sample consisted only of  $\text{Nd}_2\text{O}_3$ . During this transformation, the light-rose colour of the powder changed to light blue. When it was exposed again to atmospheric moisture and  $\text{CO}_2$ , the  $\text{Nd}_2\text{O}_3$  powder slowly became rose coloured, thus indicating the reversibility of this process. Fig. 6 shows that  $\text{Nd}_2\text{O}_3$  is characterized by a very strong IR band having the transmittance minimum at 463  $\text{cm}^{-1}$ . McDevitt and Baun [13] found the characteristic IR band for  $\text{Nd}_2\text{O}_3$  at 655  $\text{cm}^{-1}$ . Taking into account the results shown in Fig. 6, it can be concluded that McDevitt and Baun actually worked with  $\text{Nd}(\text{OH})_3$  or perhaps with  $\text{Nd}(\text{III})$ -basic carbonates.

Mullica *et al.* [14] investigated crystal structures of  $\text{Pr}(\text{OH})_3$ ,  $\text{Eu}(\text{OH})_3$  and  $\text{Tm}(\text{OH})_3$  by X-ray diffraction. The authors also observed three main regions in the corresponding IR spectra: a sharp band at  $\approx 3610 \text{ cm}^{-1}$ , a band in the region 750-650  $\text{cm}^{-1}$ ,

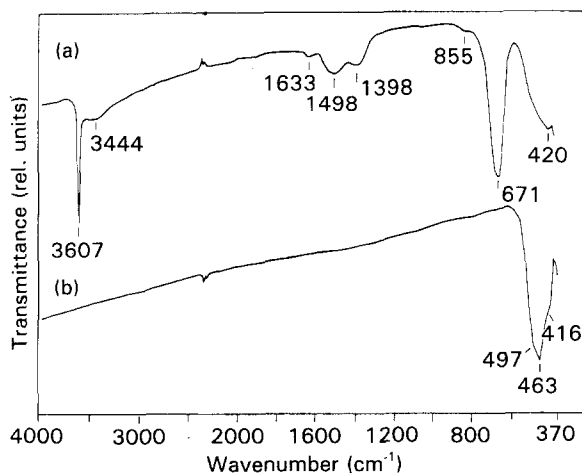


Figure 6 FT-IR spectra of (a)  $\text{Nd}_2\text{O}_3$  as-received by Trona, and (b) after calcination of this chemical at  $900^\circ\text{C}$ .

and a broad band in the region  $400\text{--}325\text{ cm}^{-1}$ . The sharp band at  $3610\text{ cm}^{-1}$  was assigned to the coordinated OH stretching, while the band found in the region  $750\text{--}650\text{ cm}^{-1}$  was assigned to the OH deformation or bending frequency. The broad band in the region  $400\text{--}325\text{ cm}^{-1}$  was attributed to the metal-oxygen stretching frequency. Brittain and Posluszny [15] found characteristic IR bands at  $3595$  and  $695\text{ cm}^{-1}$  for crystalline  $\text{Eu}(\text{OH})_3$ . With increasing heating temperature a gradual disappearance of bands at  $3595$  and  $695\text{ cm}^{-1}$  was observed, as a result of the release of water from  $\text{Eu}(\text{OH})_3$ . Takahashi and Ohtsuka [16] recorded the IR spectrum of  $\text{La}(\text{OH})_3$  and observed two bands in the region  $\approx 1500\text{--}1400$

$\text{cm}^{-1}$ , which were assigned to the splitting of the  $\nu_3(\text{CO}_3^{2-})$  frequency.

## References

1. S. MUSIĆ, in "Handbook of Ceramics and Composites", edited by N. P. Cheremisinoff, Vol. 2, (Marcel Dekker, Inc. New York, Basel, Hong Kong, 1992), Ch. 11, pp. 423-63.
2. M. RISTIĆ, S. POPOVIĆ and S. MUSIĆ, *J. Mater. Sci. Lett.* **9** (1990) 872.
3. S. MUSIĆ, V. ILAKOVAC, M. RISTIĆ and S. POPOVIĆ, *J. Mater. Sci.* **27** (1992) 1011.
4. S. MUSIĆ, S. POPOVIĆ, I. CZAKÓ-NAGY and F. GASHI, *J. Mater. Sci. Lett.* **12** (1993) 869.
5. K. RUEBENBAUER and T. BIRCHALL, *Hyperfine Int.* **7** (1979) 125.
6. M. EIBSHÜTZ, G. GORDETSKY, S. SHTRIKMAN and D. TREVÉS, *J. Appl. Phys.* **35** (1964) 1072.
7. M. RISTIĆ, S. POPOVIĆ, M. TONKOVIĆ and S. MUSIĆ, *J. Mater. Sci.* **26** (1991) 4225.
8. S. MUSIĆ, S. POPOVIĆ and M. RISTIĆ, *J. Mater. Sci.*, **28** (1993) 632.
9. M. P. ROSYNEK and D. T. MAGNUSON, *J. Catal.* **48** (1977) 417.
10. E. MATIJEVIĆ and W. P. HSU, *J. Colloid Interface Sci.* **118** (1987) 506.
11. B. AIKEN, W. P. HSU and E. MATIJEVIĆ, *J. Am. Ceram. Soc.* **71** (1988) 846.
12. M. AKINC and D. SORDELET, *Adv. Ceram. Mater.* **2** (1987) 232.
13. N. T. McDEVITT and W. L. BAUN, *Spectrochim. Acta.* **20** (1964) 799.
14. D. F. MULLICA, W. O. MILLIGAN and G. W. BEALL, *J. Inorg. Nucl. Chem.* **41** (1979) 525.
15. H. G. BRITAIN and J. V. POSLUSZNY, *Thermochim. Acta* **118** (1987) 25.
16. J. TAKAHASHI and T. OHTSUKA, *J. Am. Ceram. Soc.* **72** (1989) 426.

Received 6 August 1992

and accepted 12 August 1993